Design of Photoactivated DNA Oxidizing Agents: Synthesis and Study of Photophysical Properties and DNA Interactions of Novel Viologen-Linked Acridines

Joshy Joseph,[a] Nadukkudy V. Eldho,[a, b] and Danaboyina Ramaiah*[a]

Dedicated to Prof. Manapurathu V. George on the occasion of his 75th birthday

Abstract: A new series of photoactivated DNA oxidizing agents in which an acridine moiety is covalently linked to viologen by an alkylidene spacer was synthesized, and their photophysical properties and interactions with DNA, including DNA cleaving properties, were investigated. The fluorescence quantum yields of the viologen-linked acridines were found to be lower than that of the model compound 9-methylacridine (MA). The changes in free energy for the electron transfer reactions were found to be favorable, and the fluorescence quenching observed in these systems is explained by an electron transfer mechanism. Intramolecular electron transfer rate constants were calculated from the observed fluorescence quantum yields and singlet lifetime of MA and are in the range from $1.06\times10^{10}\ s^{-1}$ for **1a** ($n=1$) to $6\times10^{8}\ s^{-1}$ for **1c** ($n=11$), that is, the rate decreases with increasing spacer length. Nanosecond laser flash photolysis of these systems in aqueous solutions showed no transient absorption, but in the presence of guanosine or calf thymus DNA, transient absorption due to the reduced viologen radical cation was observed. Studies on DNA binding demonstrated that the viologen-linked acridines bind effectively to DNA in both intercalative and electrostatic modes. Results of PM2 DNA cleavage studies indicate that, on photoexcitation, these molecules induce DNA damage that is sensitive to formamidopyrimidine DNA glycosylase. These viologen-linked acridines are quite stable in aqueous solutions and oxidize DNA efficiently and hence can be useful as photoactivated DNA-cleaving agents which function purely by the co-sensitization mechanism.

Keywords: co-sensitizers · DNA cleavage · DNA damage · donor–acceptor systems · electron transfer

Introduction

There is widespread interest in studying the interaction of small molecules, including drugs, dyes, and toxic compounds, with DNA, as well as in the design of compounds that can cleave DNA in unique and controllable ways.[1–5] These studies not only lead to the development of molecular probes for the recognition of DNA but also provide a chemical basis for carcinogenesis and serve as model compounds for DNA–protein interactions.[6,7] Recently, there has been considerable interest in the design of photoactivated DNA cleaving agents based on intercalators, groove-binding agents, and hybrid molecules consisting of both intercalative and groove-binding moieties.[8–15] The multitude of synthetic systems used for photoinitiated oligonucleotide cleavage was recently reviewed.[16]

A number of photoactivated DNA cleaving agents, which function by different mechanisms initiated by the absorption of light, including electron transfer, generation of diffusible intermediates, and H-atom abstraction, have been reported in the literature.[16–20] The inefficiency associated with DNA cleaving agents which function by electron transfer mechanisms can be attributed to the existence of efficient electron back-transfer between the resultant oxidized nucleic acid base and the reduced sensitizer. A few examples of attempts to overcome the drawback of the electron-back-transfer processes associated with such systems, based on co-sensitization mechanisms, have been reported.[20–24] These systems consist of a sensitizer (intercalator) and a co-sensitizer (electron acceptor). On excitation, the sensitizer transfers an electron to the co-sensitizer bound on the surface of DNA. The photosensitization involving a co-sensitizer that is bound far from the sensitizer inhibits electron

[a] Dr. D. Ramaiah, J. Joseph, Dr. N. V. Eldho
Photosciences and Photonics Division
Regional Research Laboratory (CSIR)
Trivandrum 695 019 (India)
Fax: (+91) 471-249-0186 or -1712
E-mail: d_ramaiah@rediffmail.com
rama@csrrltrd.ren.nic.in

[b] Dr. N. V. Eldho
Current address: Cleveland Clinic Foundation Lerner Research Institute, Cleveland, OH 44195 (USA)

DOI: 10.1002/chem.200304936

back-transfer to some extent and thus increases the efficiency of DNA cleavage.[20] However, compounds that exhibit considerable DNA binding affinity and specificity in cleavage are yet to be achieved.

In this context, we have been interested in the design of DNA cleaving agents which can strongly bind to DNA and can induce cleavage by the co-sensitization mechanism.[25–27] Our strategy was to link an electron donor and an electron acceptor through various spacer groups and induce efficient electron transfer by changing the characteristics of the spacer (Figure 1). We chose acridine, a known intercalator,[28] as the donor and viologen as the acceptor. The excited state of the acridine chromophore can transfer an electron to the viologen moiety to give the radical cation of acridine and a reduced viologen moiety. The radical cation of acridine can oxidize DNA bases with preference for guanine and thus can initiate oxidative modification of DNA. The challenging difficulties involved are 1) generating sufficiently long lived charge-separated states so that the acridine radical cation, once formed, can oxidize the DNA base before intramolecular charge recombination takes place, and 2) achieving effective binding to DNA. Here we report the synthesis, photophysical properties, and DNA interactions of a series of viologen-linked acridines (Scheme 1). Our results indicate that the viologen-linked acridines under investigation constitute a potential group of DNA cleaving agents which function purely through the co-sensitization mechanism.

Results

Absorption properties: The absorption spectra of the viologen-linked acridine **1a** and the model compound 9-methylacridine (MA) in water are shown in Figure 2. In water, the absorption spectra of the viologen-linked acridine derivatives can be best described as the sum of absorption bands of acridine and methyl viologen (MV^{2+}). There is no evidence for any ground-state charge-transfer interaction be-

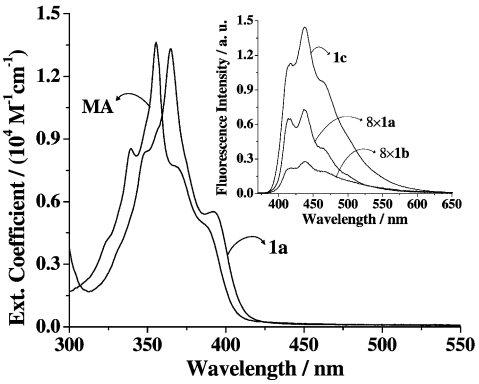

Figure 2. Absorption spectra of **1a** (4.6×10^{-5} M) and MA (5×10^{-5} M) in water. The inset shows the fluorescence emission spectra of **1a** (1.8×10^{-5} M), **1b** (2×10^{-5} M) and **1c** (2×10^{-5} M) in water. The emission spectra of **1a** and **1b** are multiplied by a factor of 8 for clarity. Excitation wavelength: 355 nm.

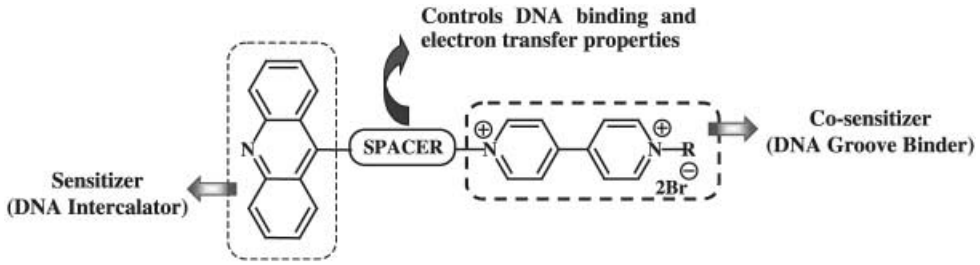

Figure 1. Schematic representation of the strategy adopted for the design of photoactivated DNA oxidizing agents.

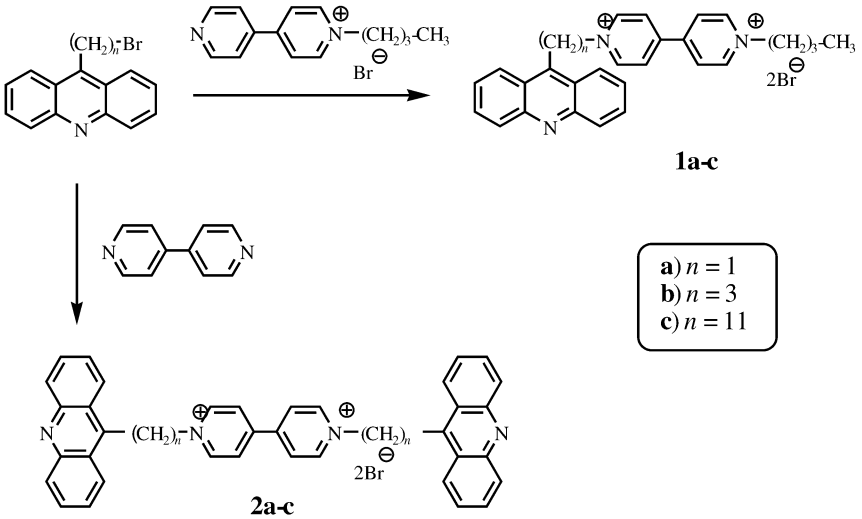

Scheme 1. Preparation of the viologen-linked acridine derivatives **1a–c** and **2a–c**.

tween the acridine and viologen moieties in these systems. However, the absorption spectra of **1a** and **2a** (CH_2 spacer) exhibited a red shift of 8–9 nm, which indicates the existence of considerable through-bond interaction between the donor and acceptor moieties (Table 1).[29] On decreasing the pH of the solution from 7 to 2, we observed a decrease in the absorption of the acridine chromophore and an increase in the absorption around 415 nm. This long-wavelength absorption

Table 1. Absorption and fluorescence emission properties of the viologen-linked acridine derivatives **1a–c** and **2a–c** and 9-methylacridine (MA) in water.

Compound	Absorption λ_{max} [nm]	Emission λ_{max} [nm]	Φ_f[a] $\times 10^2$	$k_{ET} \times 10^{10}$ s^{-1}
1a	365	437	0.7 ± 0.05	1.06
1b	358	435	0.2 ± 0.03	3.4
1c	356	436	10 ± 0.10	0.06
2a	365	437	1.2 ± 0.05	0.6
2b	356	435	0.4 ± 0.03	2.11
2c	356	435	2.5 ± 0.03	0.3
MA	355	435	55 ± 0.50	–

[a] Mean values for 2–3 independent experiments.

observed at lower pH values was attributed to the acridinium moiety formed by protonation. By monitoring the change in absorption spectra vs pH, we determined pK_a values of 3.2, 4.3, and 5.4 for **1a**, **1b**, and **1c**, respectively. The decrease in pK_a value with decreasing spacer length confirms the that considerable through-bond interactions occur between the acridine and viologen moieties in **1a**, which is therefore more acidic than **1c** ($n = 11$).

Fluorescence properties: The inset of Figure 2 shows the fluorescence emission spectra of **1a–c** in water, and Table 1 summarizes the fluorescence emission properties of **1a–c**, **2a–c**, and MA. All these compounds show structurally similar fluorescence spectra with a maximum around 435 nm. The fluorescence quantum yields of the viologen-linked acridine derivatives with short spacers ($n = 1$, 3) are two orders of magnitude smaller than that of MA. For example, **1a** and **1b** have fluorescence quantum yields of 0.007 and 0.002, while MA has a fluorescence quantum yield of 0.55. Compared to **1a** and **1b**, the corresponding bisacridine compounds **2a** and **2b** showed slightly higher fluorescence quantum yields (0.012 and 0.004, respectively). In the case of **1c** and **2c**, in which the spacer is much longer ($n = 11$), the observed fluorescence quantum yields are 0.1 and 0.025, respectively. In this case, the bis-acridine derivative **2c** is subjected to more fluorescence quenching than the mono derivative **1c**.

Electron transfer studies: The feasibility of photoinduced electron transfer between 9-methylacridine (MA) and methyl viologen (MV^{2+}) was determined by calculating the change in free energy, as well as by fluorescence titration experiments. The changes in free energy for electron transfer from the singlet excited state of MA to MV^{2+} are −1.24 and −1.27 eV in methanol and water, respectively.[26] Figure 3 shows the effect of the concentration of MV^{2+} on the fluorescence emission spectrum of MA in methanol, and the inset shows the corresponding Stern–Volmer plot. The quenching rate constant k_q was calculated by employing Equations (1) and (2), where I_0 and I are the fluorescence intensities in the absence and presence of quencher (Q), K_{sv} the Stern–Volmer constant, and τ the singlet lifetime of MA in the absence of quencher.

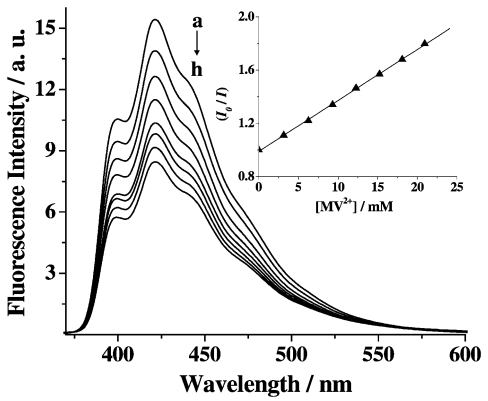

Figure 3. Effect of viologen (MV^{2+}) concentration on the fluorescence spectra of MA (2.3×10^{-5} M) in methanol. [MV^{2+}]: 0 (a), 3.2 (b), 6.3 (c), 9.3 (d), 12.3 (e), 15.2 (f), 18.1 (g) and, 21 mM (h). The inset shows the Stern–Volmer plot for the fluorescence quenching of MA by MV^{2+}. Excitation wavelength: 355 nm.

$$I_0/I = 1 + K_{sv}[Q] \quad (1)$$

$$K_{sv} = k_q \times \tau \quad (2)$$

A linear plot was obtained (inset of Figure 3), and the bimolecular quenching rate constant k_q was 4×10^{10} M^{-1} s^{-1}. Interestingly, intermolecular fluorescence quenching studies showed that the protonated form of acridine is also capable of donating an electron to MV^{2+} under light-sensitized conditions, albeit with 42 times lower efficiency than the neutral form of MA. The bimolecular rate constant for quenching of the protonated form of MA by MV^{2+}, estimated by the fluorescence titration technique, is 0.96×10^9 M^{-1} s^{-1}.

From the relative fluorescence quantum yields and the fluorescence lifetime of MA ($\tau_{ref} = 7.8$ ns in water), an estimate of the rate constant of electron transfer process k_{ET} can be made by using Equation 3 where k_{ET} is the rate of electron transfer, Φ_{ref} and Φ are the relative fluorescence quantum yields of the model compound and the viologen-linked acridine derivative, respectively, and τ_{ref} is the fluorescence lifetime of the model compound MA. The calculated intramolecular electron transfer rate constants are summarized in Table 1.

$$k_{ET} = [(\Phi_{ref}/\Phi) - 1]/\tau_{ref} \quad (3)$$

Laser flash photolysis studies: Laser flash photolysis experiments were carried out to characterize the transient intermediates involved in these systems. Figure 4 shows the tran-

sient absorption spectra obtained on laser excitation (355 nm, pulse width 20 ns) of MA in the presence of MV^{2+}. On the basis of quenching experiments with molecular oxygen, the transient species with a lifetime of 16 μs and absorption maximum at 440 nm could be assigned to the triplet excited state of MA. The other transient with two absorption maxima at 395 nm and 610 nm could be assigned to the reduced viologen radical cation, as per literature data.[30] The inset of Figure 4 shows the growth of the reduced viologen radical cation and decay of the triplet excited state of acridine. Since the formation of reduced viologen radical cation can be explained by an electron transfer process, from either the singlet or triplet excited state of MA to MV^{2+}, we examined the effect of the quencher (MV^{2+}) concentration to estimate the contributions of these two states. When the concentration of MV^{2+} used was very low (ca. 10^{-5} M), the growth of the reduced viologen radical cation was found to be concomitant with the decay of the triplet excited state of acridine. At these quencher concentrations (<25 μM), formation of the reduced viologen radical cation by quenching of the singlet excited state of acridine would therefore be less than 5%. At higher concentrations of MV^{2+} (>12 mM), the growth of the methyl viologen radical cation becomes clearly biexponential with a sudden growth immediately after the laser pulse followed by slow growth, that is, both of these excited states contribute significantly to the formation of the reduced viologen radical cation.

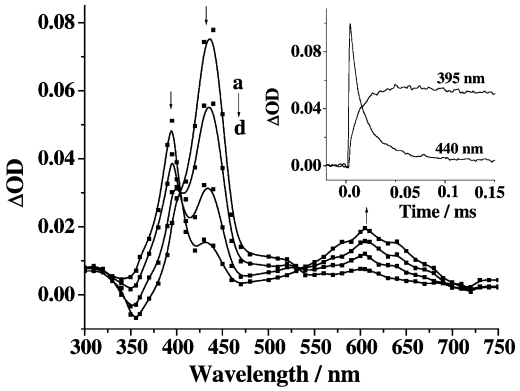

Figure 4. Transient absorption spectra of MA (5.65×10^{-5} M) in the presence of viologen (MV^{2+}, 5.85×10^{-5} M) in methanol recorded a) 7, b) 10, c) 20, and d) 40 μs after 355 nm laser excitation. The inset shows the decay of the triplet excited state of acridine at 440 nm and the growth of the reduced viologen radical cation at 395 nm.

Direct 355 nm laser excitation of the viologen-linked acridine derivatives **1a–c** and **2a–c** in water or methanol did not show any transients. However, in presence of an external donor such as guanosine or calf thymus DNA (CT DNA), characteristic transient absorption due to the reduced viologen radical cation was observed. For example, Figure 5 shows the transient absorption spectra obtained on laser excitation of **1c** ($n=11$) in the presence of CT DNA in buffered aqueous solutions. The transient absorption corresponding to the radical cation of methyl viologen exhibited second-order decay with a rate constant of $8\times10^{2}\,M^{-1}s^{-1}$.

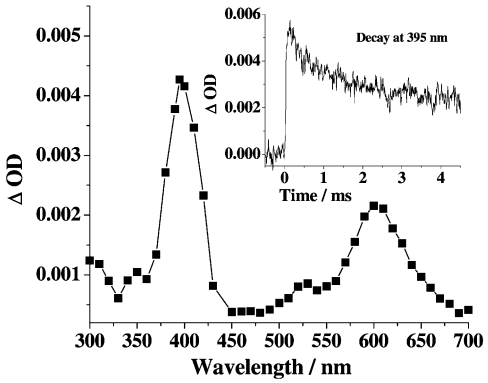

Figure 5. Transient absorption spectrum of **1c** (3.6×10^{-5} M) in the presence of CT DNA (0.33 mM) in 10 mM phosphate buffer containing 2 mM NaCl recorded 20 μs after 355 nm laser excitation. The inset shows the decay of the reduced viologen radical cation at 395 nm.

Similar observations were made for **1a**, **1b**, and **2a–c**. The formation of the reduced viologen radical cation in the presence of CT DNA indicates that these molecules are capable of oxidizing DNA efficiently.

DNA binding properties: To understand how efficiently the viologen-linked acridines interacts with DNA, we investigated their DNA binding properties with absorption and fluorescence techniques. The addition of CT DNA in small aliquots to solutions of the viologen-linked acridines resulted in a strong decrease in the absorption of the acridine chromophore and a small red shift of around 3–5 nm in each case. As a representative example, Figure 6 shows the change in absorption spectrum obtained by gradual addition of CT DNA to **1a**.

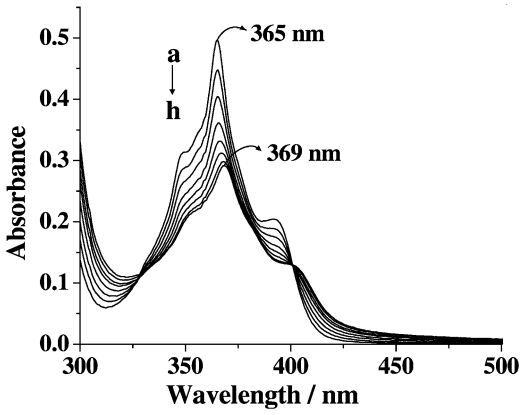

Figure 6. Absorption spectra of **1a** (3.7×10^{-5}) in the presence of CT DNA in 10 mM phosphate buffer containing 2 mM NaCl. [DNA]: 0 (a), 0.03 (b), 0.06 (c), 0.1 (d), 0.13 (e), 0.17 (f), 0.19 (g), and 0.22 mM (h).

As these molecules are donor–acceptor systems, the fluorescence spectral properties showed an interesting variation. On addition of CT DNA to a solution of **1a**, an initial enhancement (Figure 7) followed by a strong quenching (inset of Figure 7) of the fluorescence emission was observed. Similar observations were made for **1b**, whereas **1c**

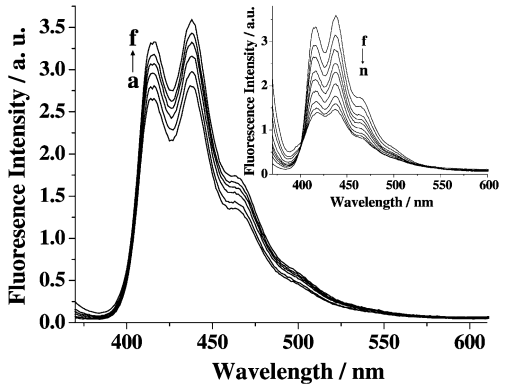

Figure 7. Fluorescence spectra of **1a** (3.7×10^{-5} M) in the presence of CT DNA in 10 mM phosphate buffer containing 2 mM NaCl. [DNA]: 0 (a), 0.03 (b), 0.06 (c), 0.1 (d), 0.13 (e), 0.22 mM (f); The inset shows [DNA] 0.22 (f), 0.32 (g), 0.47 (h), 0.61 (i), 0.75 (j), 0.89 (k), 1.4 (l), 1.85 (m), and 2.45 mM (n). Excitation wavelength: 355 nm.

($n=11$) showed a regular decrease in fluorescence yield on addition of CT DNA. The viologen-linked bis-acridine derivatives **2a–c** in the presence of CT DNA, on the other hand, behaved similarly to the mono-acridine analogues **1a–c**.

The fluorescence spectral changes observed in the presence of CT DNA were analyzed and fitted to the noncooperative model of McGhee and von Hippel to obtain the DNA association constants.[31–33] As representative examples, the Scatchard plots for **1a** and **1c** are shown in Figure 8, and the DNA association constants are summarized in Table 2. The DNA association constants of the viologen-linked acridine derivatives depend on the salt concentration and the length of the spacer. For example, **1a** has an association constant of 9.24×10^5 M^{-1} in 10 mM phosphate buffer containing 2 mM NaCl, whereas in the presence of 100 mM NaCl, a lower value of 1×10^5 M^{-1} was observed. Compound **1c** exhibited higher affinity for DNA (5.24×10^6 M^{-1}) relative to **1a**. The rate constants k_{DNA} for the quenching of the singlet excited state of the acridine chromophore in the viologen-linked acridine derivatives in the presence of DNA were evaluated on the basis of the limiting fluorescence intensity (under conditions for which 99% of the substrate is bound to DNA) and by using Equation (4)[24] where I_0 and I are the fluorescence intensities in the absence and presence of DNA, and k_{SI} is the sum of rate constants (k_d+k_{ET}) for deactivation of the singlet state.

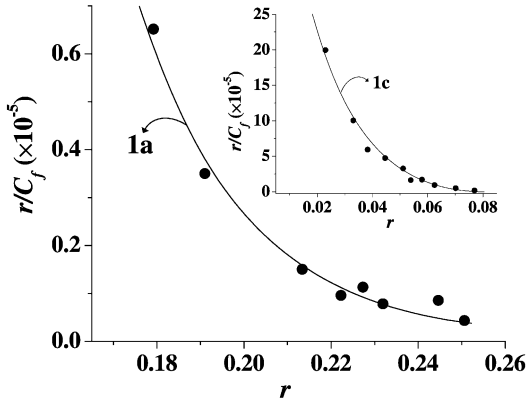

Figure 8. Scatchard plot for the binding of **1a** to CT DNA in 10 mM phosphate buffer containing 2 mM NaCl. The inset shows the Scatchard plot for **1c** under similar conditions.

Table 2. DNA association constants K, site-exclusion parameters n, and singlet deactivation rates of the viologen-linked acridines.[a]

Compd	Ionic strength	K [M^{-1}]	n[b]	k_{SI}[c] [s^{-1}]	k_{DNA}[d] [s^{-1}]
1a	2 mM NaCl	9.24×10^5	4	1.1×10^{10}	0.98×10^{10}
	100 mM NaCl	1.01×10^5	11		
1c	2 mM NaCl	5.24×10^6	7	7.3×10^8	0.52×10^{10}
	100 mM NaCl	1.64×10^5	15		
2a	2 mM NaCl	1.30×10^6	5	6.1×10^9	0.65×10^{10}
	100 mM NaCl	3.90×10^5	14		
2c	2 mM NaCl	2.2×10^6	9	3.1×10^9	0.87×10^{10}
	100 mM NaCl	2.1×10^5	18		

[a] Determined in 10 mM phosphate buffer (pH 7.4) containing 2 or 100 mM NaCl. [b] Number of nucleotides occluded by a bound ligand. [c] Taken as the sum of the radiative and nonradiative rate constants (k_d) for deactivation of the singlet excited state of acridine and the rate constant for intramolecular electron transfer from acridine to viologen (k_{ET}). [d] Calculated as per the equation reported in reference [24].

$$I_0/I = 1 + k_{DNA}/k_{SI} \quad (4)$$

The k_{DNA} values obtained for these compounds are summarized in Table 2.

Binding selectivity of the viologen-linked acridine derivatives was analyzed by employing polynucleotides such as poly(dA).poly(dT) and poly(dG).poly(dC). Figure 9 shows the effect of poly(dA).poly(dT) concentration on the fluorescence emission spectrum of **1a**, while the inset shows the effect of poly(dG).poly(dC). A strong enhancement in the fluorescence emission was observed in the case of **1a** with increasing concentration of poly(dA).poly(dT). A similar observation was made for **1c**. However, the negligible effect of the polynuleotide poly(dG).poly(dC) on the absorption

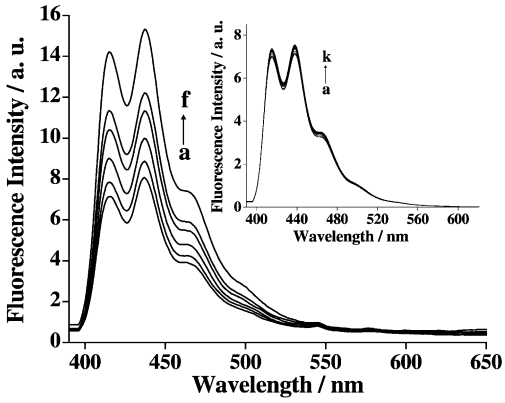

Figure 9. Fluorescence spectra of **1a** (1.2×10^{-5} M) in the presence of poly(dA).poly(dT) in 10 mM phosphate buffer containing 2 mM NaCl. [poly(dA).poly(dT)]: 0 (a), 0.4 (b), 1.3 (c), 2.2 (d), 4.6 (e), and 20 μM (f). The inset shows the fluorescence emission spectra of **1a** (1.1×10^{-5} M) in the presence of poly(dG).poly(dC) under similar conditions. [poly(dG).poly(dC)]: 0 (a), 0.2 (b), 2.3 (c), 3.2 (d), 5.0 (e), 6.5 (f), 7.2 (g), 8.5 (h), 9.7 (j), and (k) 11.0 μM. Excitation wavelength: 355 nm.

and fluorescence properties indicates preferential affinity of the viologen-linked acridine derivatives to the former sequences.

DNA cleaving properties: To understand the efficiency and nature of oxidative DNA damage induced by the viologen-linked acridines, we examined the cleavage of supercoiled DNA from bacteriophage PM2 (PM2 DNA, 10^4 bp) in the presence and absence of various repair endonucleases.[34–36] Phosphate-buffered (pH 7.4) solutions of PM2 DNA (10 μg mL^{-1}) at 0 °C were irradiated with 360 nm light in the presence of various concentrations of **1a** and **1c**. Subsequently, the DNA was analyzed for the following types of modifications: 1) single- and double-strand DNA breaks; 2) sites of base loss (AP sites) recognized by exonuclease III; 3) base modifications plus AP sites sensitive to T4 endonuclease V; 4) base modifications plus AP sites sensitive to endonuclease III; and 5) base modifications plus AP sites sensitive to formamidopyrimidine DNA glycosylase (FPG protein).

The results of various modifications induced by the photoactivated viologen linked acridines **1a** and **1c** in the form of damage profiles are shown in Figure 10. It is evident from the damage profiles that both these compounds induced

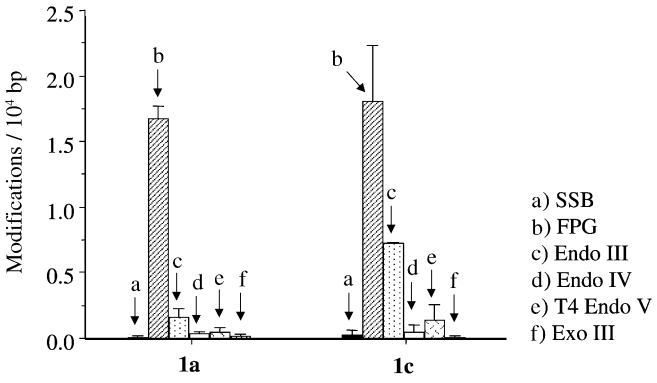

Figure 10. DNA damage profiles showing single-strand breaks (SSB) and various endonuclease-sensitive modifications induced in PM2 DNA by photoactivated **1a** (250 nM, 18 kJ m^{-2}) and **1c** (1 μM, 9 kJ m^{-2}).

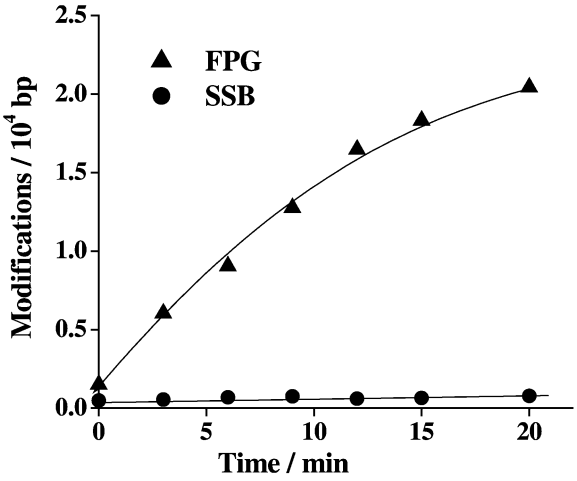

Figure 11. Time dependence of single-strand breaks (SSB) and FPG-sensitive modifications, induced in PM2 DNA by **1a** (0.25 μM, 0 °C) on UV irradiation with 360 nm light (4.6 kJ m^{-2}).

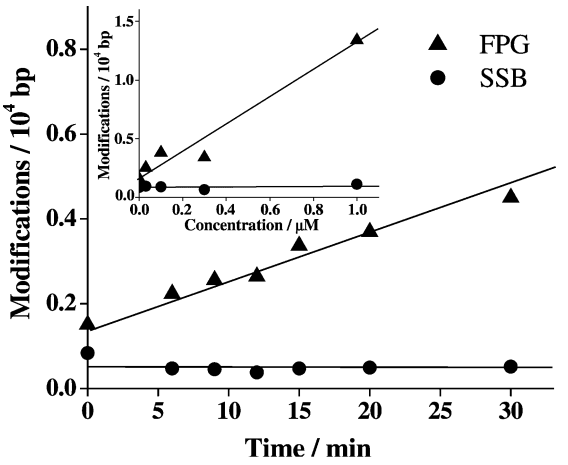

Figure 12. Time dependence of single-strand breaks (SSB) and FPG-sensitive modifications induced in PM2 DNA by **1c** (0.30 μM, 0 °C) upon UV irradiation with 360 nm light (4.6 kJ m^{-2}). The inset shows the concentration dependence of SSB and FPG-sensitive modifications induced in PM2 DNA by **1c** on UV irradiation with 360 nm light (4.6 kJ m^{-2}).

very few AP sites and few modifications sensitive to endonuclease III, but a large number of base modifications sensitive to FPG protein. Compound **1a** ($n=1$) was about four times more efficient in inducing DNA damage than **1c** ($n=11$). However, no single-strand breaks (SSB) were observed in each case. Since the FPG protein recognizes the major damage, we investigated the effect of irradiation time and concentration on the formation of FPG-sensitive modifications and SSBs induced by **1a** (Figure 11) and **1c** (Figure 12). In each case, the damage sensitive to FPG protein increases with increasing irradiation time. No significant increase in SSBs was observed, even after irradiation for 30 min. Similarly, an increase in FPG-sensitive modifications was observed with increasing concentration of **1c** (inset of Figure 12). Furthermore, no significant DNA damage was observed on irradiation of PM2 DNA alone or in presence of viologen, or in the dark in presence of the viologen-linked acridine derivatives at high concentrations, and this indicates that the DNA damage observed is purely caused by photoactivated viologen-linked acridine systems.

Discussion

For compounds in which a donor and an acceptor are separated by flexible or rigid spacer groups the dependence of electron transfer reactions on distance is well documented.[37–40] In such systems, both through-bond and through-space interactions play a role in determining the photophysical properties. In the case of the viologen-linked acridines and bisacridines, the observed fluorescence quantum yields were very low compared to that of the model compound

MA. For example **1a**, in which the spacer is a single methylene group, showed a higher degree of fluorescence quenching than the compound with the longer spacer **1c** ($n=11$). This indicates that the through-bond interactions are at a maximum for **1a**, while the through-space interactions play significant role in **1c**. On the other hand, in **1b**, in which the spacer length is medium ($n=3$), we observed maximum fluorescence quenching, which may result from the cumulative effect of through-bond and through-space interactions between the donor and acceptor groups. The calculated changes in free energy and the results of intermolecular fluorescence quenching experiments showed that the acridine chromophore can act as an efficient electron donor to the viologen moiety. We observed a value of $k_{ET}=1.06\times 10^{10}\,s^{-1}$ for **1a** ($n=1$), whereas **1c**, with the longer spacer ($n=11$), exhibited value around 15 times lower ($k_{ET}=6.4\times 10^{8}\,s^{-1}$, Table 1), which indicates a decrease in intramolecular electron transfer rate with increasing spacer length.

As observed in the laser flash photolysis studies, both the singlet and triplet excited states of MA can transfer an electron to MV^{2+} to form the reduced methyl viologen radical cation. In the viologen-linked acridines, the rate of charge separation k_{ET} and the rate of charge recombination are expected to be fast, and hence the reduced viologen radical cation could not be observed by a nanosecond laser flash photolysis technique. However, in the presence of an external donor such as guanosine or DNA, we observed the formation of the reduced methyl viologen radical cation. This can be attributed to the enhanced lifetime of the charge-separated species in the presence of a sacrificial donor.

We observed a strong hypochromic effect in the absorption spectra of the viologen-linked acridines in the presence of DNA, as reported for molecules that undergo intercalative interactions with DNA.[28] However, we observed that the spacer length and electrostatic interactions also contribute to the stability of the viologen-linked acridine–DNA complexes. The involvement of electrostatic interactions was supported by the fact that the DNA association constants were reduced by nearly one order of magnitude when the salt concentration was varied from 2 to 100 mM. Interestingly, these compounds exhibited unusual fluorescence emission properties in the presence of DNA. Initial concentrations of added CT DNA (<0.2 mM) resulted in an enhancement of fluorescence quantum yields of the viologen-linked acridines ($n=1$, 3), which was followed by strong quenching of the fluorescence at higher concentrations of DNA. As these molecules are donor–acceptor systems, their fluorescence properties in the presence of DNA could be controlled by several factors. Of these, the predominant factor would be the perturbation of the interactions between the acridine and viologen moieties in the presence of DNA. At lower concentrations of DNA, perturbation of interactions between the acridine and viologen moiety results in enhancement of fluorescence yields. However, at higher concentrations of DNA, for which more than 95% of the molecules are intercalated between the base pairs of DNA, the electron transfer processes from DNA bases become more predominant, and this results in strong fluorescence quenching of these systems.

Considering the electron transfer processes in the presence of DNA, two pathways can be proposed for the formation of the reduced viologen radical cation, as shown in Figure 13.

In path A electron transfer from the DNA base (preferably from guanine) to the excited acridine moiety is followed by transfer of an electron from the acridine radical anion to the viologen moiety with formation of the charge-separated radical cation of viologen. In path B electron transfer from the excited acridine moiety is followed by the reduction of the acridine radical cation by DNA base. The efficiency of these two pathways in the viologen-linked acridine derivatives was evaluated in terms of the k_{DNA} values and other singlet deactivation processes [Eqs. (5) and (6)],[24] where Φ_A and Φ_B are the efficiencies for paths A and B, respectively, k_{DNA} and k_{ET} the rate constants for the quenching of the singlet excited state of acridine by DNA and covalently linked viologen, respectively (data shown in Table 1 and Table 2), and k_d is the intrinsic rate constant for the deactivation of the singlet excited state of acridine ($k_d = 1.28\times 10^{8}\,s^{-1}$).

$$\Phi_A = k_{DNA}/(k_{ET}+k_{DNA}+k_d) \quad (5)$$

$$\Phi_B = k_{ET}/(k_{ET}+k_{DNA}+k_d) \quad (6)$$

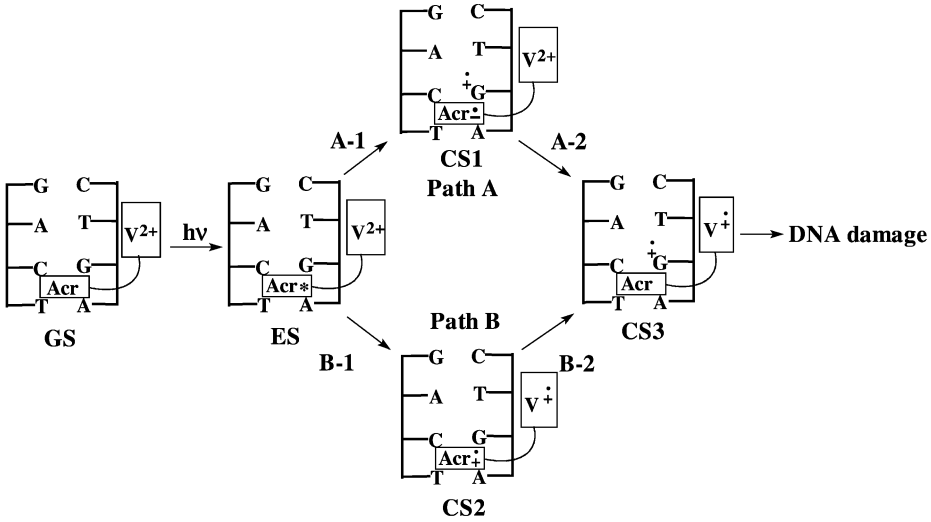

Figure 13. Schematic representation of paths A and B for oxidative DNA damage induced by photoactivated viologen-linked acridine derivatives (Acr = acridine moiety, V = viologen moiety, GS = ground-state complex, ES = excited-state complex, CS = charge-separated state).

In the case of **1a** ($n=1$), it was observed that both path A and path B contribute equally to deactivation of the singlet state of acridine, whereas path A was the predominant process (>90%) for **1c** ($n=11$). Both these mechanisms finally lead to the formation of the charge-separated radical cation of methyl viologen and the radical cation of the nucleic acid base.

The PM2 DNA damage analysis confirms that the charge-separated base radical cation, once formed, can result in the oxidative DNA damage. It was furthermore observed that most of the DNA damage induced by these systems was recognized by FPG protein,[34] which is known to recognize oxidized DNA products such as 8-hydroxyguanosine and formamidopyrimidines, which can be formed by an electron transfer mechanism.[34–36] The possibility of involvement of singlet oxygen and hydroxyl radical intermediates can be ruled out, since the viologen-linked acridine derivatives exhibited negligible triplet excited states, and the damage profiles observed are quite different from that induced by the disodium salt of 1,4-etheno-2,3-benzoxlioxin-1,4-dipropanoic acid ($NDPO_2$) and ionizing radiation.[41,42] These results clearly indicate the fact that the DNA modifications induced by these molecules originate from the oxidation of guanosine. Since guanine has the lowest ionization potential, it can be preferentially oxidized by the excited state of the acridine chromophore of these compounds. Moreover, the selective oxidation of guanine in DNA can also be rationalized by the mechanism of fast hole hopping[43,44] even if the initial electron transfer caused by the photoexcited viologen-linked acridine occurs at a remote site in the DNA duplex.

Conclusion

The absorption spectra of the viologen-linked acridines in water closely resemble those of the model compounds 9-methylacridine (MA) and viologen, and this indicates the absence of ground-state interactions between the viologen and acridine units. The lower fluorescence quantum yields of the viologen-linked acridines relative to MA, suggest that the fluorescence of acridine is efficiently quenched by the viologen moiety, and that electron transfer is the predominant nonradiative decay pathway. Laser excitation (355 nm) of these systems in the presence of external donors such as guanosine or DNA showed transients due to the reduced viologen radical cation. The calculated k_{DNA} and k_{ET} values indicate that both paths A and B, involving the reduction and oxidation of the excited state of acridine by DNA and the viologen moiety, respectively, are important, and the predominance of these pathways depends on the spacer length. Both these pathways result in the charge-separated reduced viologen radical cation and the radical cation of the nucleic acid base and cause DNA modifications that are sensitive to FPG protein. Results of these investigations indicate that this new series of bifunctional compounds, which are stable in aqueous medium and efficient in oxidizing guanosine and DNA, can have potential use as photoactivated DNA oxidizing agents that function purely by the co-sensitization mechanism.

Experimental Section

General techniques: The equipment and procedure for melting point determination and recording spectra are described in earlier publications.[45,46] An Elico pH meter was used for pH measurements. The fluorescence quantum yields were determined by using optically matched solutions. 9-Aminoacridine in methanol ($\Phi_f=0.99$) was used as standard.[47] The fluorescence lifetimes were measured on an Edinburgh FL900CD single-photon counting system and were determined by deconvoluting the instrumental function with a mono- or biexponential decay and minimizing the χ^2 values of the fit to 1 ± 0.1. Laser flash photolysis experiments were carried out in an Applied Photophysics Model LKS-20 Laser Kinetic Spectrometer using the third harmonic (355 nm) of a Quanta Ray GCR-12 series pulsed Nd:YAG laser. Cyclic voltammetry was performed on a BAS CV50W Cyclic Voltammeter with tetrabutylammonium tetrafluoroborate as supporting electrolyte in dry acetonitrile. A standard three-electrode configuration was used with a glassy carbon working electrode, a platinum auxiliary electrode, and a Ag/AgCl (3 M NaCl) reference electrode. The potentials were calibrated against the standard calomel electrode (SCE). The DNA binding studies were carried out in 10 mM phosphate buffer containing 2 or 100 mM NaCl. The absorption and fluorescence titrations of the viologen-linked acridines with DNA were carried out by adding small aliquots of DNA solution containing the same concentration of the compound as in the test solution. The binding affinities were calculated from fluorescence quantum yields according to the method of McGhee and von Hippel by using the data points of the Scatchard plot.[31–33] For compounds **1a,b** and **2a,b**, only data that showed regular fluorescence quenching on addition of DNA were used for the calculation of DNA association constants.

Materials: 4,4′-Bipyridine and methyl viologen dichloride hydrate (MV^{2+}; 98%) were purchased from Aldrich and used as received. Calf thymus DNA (CT DNA), poly(dA).poly(dT) and poly(dG).poly(dC) were obtained from the Pharmacia Biotech (USA). Solutions of CT DNA were sonicated for 1 h and filtered through a 0.45 μm Millipore filter. The concentrations of DNA solutions were determined by using the molar absorptivities $\varepsilon=6600\,M^{-1}cm^{-1}$ at $\lambda_{max}=260$ nm for CT DNA; $\varepsilon=6000\,M^{-1}cm^{-1}$ at $\lambda_{max}=260$ nm for poly(dA).poly(dT), and $\varepsilon=7400\,M^{-1}cm^{-1}$ at $\lambda_{max}=253$ nm for poly(dG).poly(dC).[48] DNA from bacteriophage PM2 (PM2 DNA) was prepared according to the method of Salditt et al.[49] More than 95% was in the supercoiled form, as determined by the reported method. Formamidopyrimidine DNA glycosylase[50] was obtained from Dr. S. Boiteux. Endonuclease was provided by Dr. R. P. Cunningham.[51] T4 endonuclease V was partially purified by the method of Nakabeppu et al.[52] Exonuclease III was purchased from Boehringer. All repair endonucleases were tested for their incision at reference modifications under the applied assay conditions to ensure that the correct substrate modifications are fully recognized and no incisions at nonsubstrate modifications take place.

1-Butyl-4,4′-bipyridinium bromide was obtained in 95% yield by the reaction of 4,4′-bipyridine with 1-bromobutane in the molar ratio 3:1 in dry acetonitrile. 9-Methylacridine (MA), m.p. 114–115 °C (lit. m.p. 115–116 °C),[53] 9-bromomethylacridine, m.p. 160–161 °C (lit. m.p. 160–161 °C),[53] 3-(acridin-9-yl)-1-bromopropane, m.p. 103–104 °C (lit. m.p. 104–105 °C),[54,55] and 11-(acridin-9-yl)-1-bromoundecane, m.p. 58–59 °C (lit. m.p. 58–59 °C),[54,55] were synthesized as per reported procedures.

Synthesis of monofunctional viologen-linked acridine derivatives 1a–c: A solution of ω-(acridin-9-yl)-α-bromoalkane (1 mmol) and 1-butyl-4,4′-bipyridinium bromide (1 mmol) in dry acetonitrile (30 mL) was stirred at 30 °C for 12 h. The precipitated solid was collected by filtration and washed with dry acetonitrile and dichloromethane to remove unchanged starting material. The solid that remained was further purified by Soxhlet extraction with dichloromethane and recrystallized from ethyl acetate/acetonitrile (4/1) to give **1a–c** in good yields.

1-[(Acridin-9-yl)methyl]-1′-butyl-4,4′-bipyridinium dibromide (1a): 67% yield, m.p. 260–261 °C; ^{1}H NMR (300 MHz, [D$_6$]DMSO, 30 °C, TMS): δ = 0.91 (t, J = 7.3 Hz, 3H, CH_3), 1.26–1.33 (m, 2H, CH_2), 1.89–1.94 (m, 2H, CH_2), 4.66 (t, J = 7.3 Hz, 2H, CH_2), 7.11 (s, 2H, CH_2), 7.78 (t, J = 7.6 Hz, 2H, Ar–H), 7.97 (t, J = 7.6 Hz, 2H, Ar–H), 8.32 (d, J = 8.7 Hz, 2H, Ar–H), 8.53 (d, J = 8.7 Hz, 2H, Ar–H), 8.59 (d, J = 6.4 Hz, 2H, Ar–H), 8.66 (d, J = 6.3 Hz, 2H, Ar–H), 9.18 (d, J = 6.4 Hz, 2H, Ar–H), 9.31 ppm (d, J = 6.4 Hz, 2H, Ar–H); ^{13}C NMR (75 MHz, [D$_6$]DMSO, 30 °C, TMS): δ = 149.8, 148.5, 146.0, 145.7, 131.4, 131.0, 130.2, 128.7, 127.1, 126.9, 126.0, 124.4, 121.4, 61.1, 55.4, 33.0, 19.1, 13.7 ppm; HRMS (ESI) calcd for $C_{28}N_3H_{27}Br$: 484.1372; found: 484.1378; elemental analysis (%) calcd for $C_{28}H_{27}Br_2N_3$: C 59.49, H 4.81, N 7.43; found: C 59.28, H 4.98, N 7.31.

1-[3-(Acridin-9-yl)propyl]-1′-butyl-4,4′-bipyridinium dibromide (1b): 71% yield, m.p. 253–254 °C; ^{1}H NMR (300 MHz, [D$_6$]DMSO, 30 °C, TMS): δ = 0.94 (t, J = 7.4 Hz, 3H, CH_3), 1.28–1.40 (m, 2H, CH_2), 1.92–2.02 (m, 2H, CH_2), 2.46–2.51 (m, 4H, CH_2), 3.95 (t, J = 7.4 Hz, 2H, CH_2), 4.74 (t, J = 7.3 Hz, 2H, CH_2), 7.80 (t, J = 8.2 Hz, 2H, Ar–H), 8.05 (t, J = 7.3 Hz, 2H, Ar–H), 8.28 (d, J = 8.6 Hz, 2H, Ar–H), 8.71 (d, J = 8.6 Hz, 2H, Ar–H), 8.83–8.86 (m, 4H, Ar–H), 9.46 (d, J = 6.3 Hz, 2H, Ar–H), 9.57 ppm (d, J = 6.3 Hz, 2H, Ar–H); ^{13}C NMR (75 MHz, [D$_6$]DMSO, 30 °C, TMS): δ = 149.5, 149.3, 146.2, 145.4, 133.3, 127.5, 127.2, 125.9, 125.0, 61.5, 60.7, 33.2, 33.2, 24.8, 19.3, 13.8 ppm; MS (FAB): m/z (%): 433 [M^+] (10), 376 (2); elemental analysis (%) calcd for $C_{30}H_{31}Br_2N_3$: C 60.72, H 5.27, N 7.08; found: C 60.51, H 5.21, N 7.27.

1-[11-(Acridin-9-yl)undecyl]-1′-butyl-4,4′-bipyridinium dibromide (1c): 65% yield, m.p. 248–249 °C; ^{1}H NMR (300 MHz, [D$_6$]DMSO, 30 °C, TMS): δ = 0.95 (t, J = 7.3 Hz, 3H, CH_3), 1.23–1.71 (m, 18H, $(CH_2)_9$), 1.95–1.98 (m, 4H, CH_2CH_2), 3.65 (t, J = 7.3 Hz, 2H, CH_2), 4.74 (t, J = 7.3 Hz, 4H, CH_2), 7.65 (t, J = 7.6 Hz, 2H, Ar–H), 7.85 (t, J = 7.6 Hz, 2H, Ar–H), 8.14 (d, J = 8.6 Hz, 2H, Ar–H), 8.38 (d, J = 8.6 Hz, 2H, Ar–H), 8.82 (d, J = 6.4 Hz, 4H, Ar–H), 9.43 ppm (d, J = 6.4 Hz, 4H, Ar–H); ^{13}C NMR (75 MHz, [D$_6$]DMSO, 30 °C, TMS): δ = 149.0, 148.3, 147.7, 146.1, 130.5, 130.1, 127.0, 126.2, 125.1, 124.7, 61.3, 61.0, 33.1, 31.6, 31.2, 29.7, 29.3, 29.1, 28.8, 27.1, 25.8, 19.2, 13.7 ppm; MS (FAB): m/z (%): 545 [M^+] (10), 488 (1); elemental analysis (%) calcd for $C_{38}H_{47}Br_2N_3$: C 64.68, H 6.71, N 5.98; found: C 64.42, H 6.44, N 5.72.

Synthesis of the bifunctional viologen-linked acridine derivatives 2a–c: A solution of ω-(acridin-9-yl)-α-bromoalkane (2 mmol) and 4,4′-bipyridine (1 mmol) in dry acetonitrile (90 mL) was stirred at 30 °C for 12 h. The precipitated solid was collected by filtration and washed with dichloromethane and acetonitrile. Soxhlet extraction of the solid with dichloromethane and recrystallization from ethyl acetate/acetonitrile (4/1) gave **2a–c** in quantitative yield.

Bis-1,1′-[(acridin-9-yl)methyl]-4,4′-bipyridinium dibromide (2a): 80% yield, m.p. >400 °C; ^{1}H NMR (300 MHz, [D$_6$]DMSO, 30 °C, TMS): δ = 7.09 (s, 4H, CH_2), 7.77–7.95 (m, 8H, Ar–H), 8.21–8.55 (m, 16H, Ar–H), 9.05–9.16 ppm (m, 8H, Ar–H); ^{13}C NMR (75 MHz, [D$_6$]DMSO, 30 °C, TMS): δ = 150.9, 149.7, 148.5, 145.4, 133.9, 131.3, 128.8, 127.6, 126.4, 124.5, 58.5 ppm; HRMS (ESI) calcd for $C_{38}N_4H_{28}Br$: 619.1498; found: 619.1503; elemental analysis (%) calcd for $C_{38}H_{28}Br_2N_4$: C 65.16, H 4.03, N 8.00; found: C 64.98, H 3.79, N 7.91.

Bis-1,1′-[3-(acridin-9-yl)propyl]-4,4′-bipyridinium dibromide (2b): 75% yield, m.p. 223–224 °C; ^{1}H NMR (300 MHz, D_2O, 30 °C) δ = 2.50–2.60 (m, 4H, CH_2), 3.96 (t, J = 7.4 Hz, 4H, CH_2), 4.88 (t, J = 7.4 Hz, 4H, CH_2), 7.79–7.83 (m, 6H, Ar–H), 8.01–8.07 (m, 8H, Ar–H), 8.26 (d, J = 6.3 Hz, 2H, Ar–H), 8.46–8.48 (m, 4H, Ar–H), 8.68–8.71 (m, 2H, Ar–H), 8.93 ppm (d, J = 6.3 Hz, 2H, Ar–H); ^{13}C NMR (75 MHz, [D$_6$]DMSO, 30 °C, TMS): δ = 150.8, 148.4, 145.8, 132.7, 126.8, 126.5, 125.5, 125.3, 124.4, 121.9, 60.3, 32.4, 24.3 ppm; MS (FAB): m/z (%): 596[M^+] (1), 376 (10); elemental analysis (%) calcd for $C_{42}H_{36}Br_2N_4$: C 66.68, H 4.80, N 7.41; found: C 66.49, H 4.91, N 7.21.

Bis-4,4′-[11-(acridin-9-yl)undecyl]bipyridinium dibromide (2c): 46% yield, m.p. 152–153 °C; ^{1}H NMR (300 MHz, [D$_6$]DMSO, 30 °C, TMS): δ = 1.22–1.94 (m, 36H, $(CH_2)_9$), 3.64 (t, J = 7.3 Hz, 4H, CH_2), 4.64 (t, J = 7.3 Hz, 4H, CH_2), 7.65 (t, J = 7.6 Hz, 4H, Ar–H), 7.85 (t, J = 7.6 Hz, 4H, Ar–H), 8.04 (d, J = 5.8 Hz, 4H, Ar–H), 8.15 (d, J = 8.6 Hz, 4H, Ar–H), 8.38 (d, J = 8.6 Hz, 2H, Ar–H), 8.63 (d, J = 6.3 Hz, 2H, Ar–H), 8.87 (d, J = 5.8 Hz, 2H, Ar–H), 9.24 ppm (d, J = 6.3 Hz, 2H, Ar–H); ^{13}C NMR (75 MHz, [D$_6$]DMSO, 30 °C, TMS): δ = 151.4, 148.4, 147.6, 145.7, 130.5, 130.1, 126.2, 125.8, 125.1, 122.3, 60.8, 31.6, 31.1, 29.7, 29.3, 29.1, 28.8, 27.1, 25.8 ppm; MS (FAB): m/z (%): 820 [M^+] (1), 488 (10); elemental analysis (%) calcd for $C_{58}H_{68}Br_2N_4$: C 71.01, H 6.99, N 5.71; found: C 70.88, H 6.67, N 5.92.

Free-energy calculations: The change in free energy of photoinduced electron transfer ΔG_{el} was calculated with the Rehm–Weller equation [Eq. (7)],[56,57] where $E^0_{(D)}$ is the oxidation potential of the donor, $E^0_{(A)}$ the reduction potential of the acceptor, $E_{(0,0)}$ the excitation energy of the sensitizer, ε_s the dielectric constant of the solvent used, r_D and r_A are the radii of the donor and acceptor molecules, and d_{cc} is the center-to-center distance between the ions.

$$\Delta G_{el} = E^0_{(D)} - E^0_{(A)} - E_{(0,0)} - \frac{e^2}{2}\left(\frac{1}{r_D}+\frac{1}{r_A}\right)\left(\frac{1}{37}-\frac{1}{\varepsilon_S}\right) - \frac{e^2}{\varepsilon_S d_{cc}} \quad (7)$$

The values of r_D, r_A, and d_{cc} were estimated by using a computer modeling program.[58] The free-energy change for electron transfer from the singlet excited state of acridine to viologen was calculated from the measured oxidation potential of MA (1.6 V versus SCE),[26] the reduction potential of methyl viologen (−0.45 eV versus SCE),[59] and the singlet energy of acridine (3.26 eV).[60] The change in free energy for electron transfer from the excited state of the protonated acridine moiety ($E_{0,0}$ = 2.8 eV)[60] to methyl viologen was not calculated due to the lack of the one-electron oxidation potential of the donor.

DNA damage analysis: The exposure of PM2 DNA (10 μg mL^{-1}) to near-UV radiation (360 nm) in the presence and absence of the viologen-linked acridine derivatives was carried out on ice in phosphate buffer (5 mM KH_2PO_4, 50 mM NaCl, pH 7.4) by means of a black light lamp (Osram HQV; 5 min at 10 cm distance). The modified DNA was precipitated by ethanol/sodium acetate and redissolved in BE1 buffer (20 mM Tris-HCl, pH 7.5, 100 mM NaCl, 1 mM EDTA), and the DNA damage was quantified by means of various endonucleases and DNA relaxation assay, as reported earlier.[34,35]

Acknowledgement

We are highly grateful to Professor B. Epe for his helpful suggestions and for help in carrying out DNA cleaving experiments. Support from the Department of Science and Technology, Government of India and the Council of Scientific and Industrial Research (CSIR) is gratefully acknowledged. This is contribution no. RRLT-PPD(PRU)-152 from the Regional Research Laboratory, Trivandrum.

[1] N. Bischofberger, R. G. Shea in *Nucleic Acid Targeted Drug Design* (Eds.: C. L. Propst, T. J. Perun), Dekker, New York, **1992**, pp. 579–612.
[2] D. M. Tidd in *Molecular Aspects of Anticancer Drug-DNA Interactions, Vol. 1* (Eds.: S. Neidle, M. Waring), CRC, Boca Raton, FL, **1993**, pp. 272–300.
[3] J. K. Barton, *Bioinorganic Chemistry*, University Science Books, Mill Vally, CA, **1994**, pp. 455–503.
[4] W. D. Wilson, R. L. Jones in *Intercalator Chemistry* (Eds.: M. S. Whittingham, A. J. Jacobson), Academic Press, New York, **1982**, pp. 445–474.
[5] *Small Molecule DNA and RNA Binders* (Eds.: M. Demeunynck, C. Bailly, W. D. Wilson), Wiley-VCH, Weinheim, **2003**.
[6] S. J. Lippard in *Bioorganic Chemistry*, University Science Books, Mill Vally, CA, **1994**, pp. 505–583.
[7] B. Pullman, J. Jortner, *Molecular Basis of Specificity in Nucleic Acid-Drug Interactions, Vol. 1*, CRC Press, Ann Arbor, MI, **1993**.
[8] B. Armitage, C. Yu, C. Devadoss, G. B. Schuster, *J. Am. Chem. Soc.* **1994**, *116*, 9847–9859.
[9] R. E. Holmlin, P. J. Dandliker, J. K. Barton, *Angew. Chem.* **1997**, *109*, 2830–2848; *Angew. Chem. Int. Ed. Engl.* **1997**, *36*, 2714–2730.
[10] C. V. Kumar, E. H. A. Punzalan, W. B. Tan, *Tetrahedron* **2000**, *56*, 7027–7040.
[11] W. D. Wilson, L. Ratmeyer, M. Zhao, L. Strekovski, D. Boykin, *Biochemistry* **1993**, *32*, 4098–4104.

[12] P. E. Nielsen, *Bioconjugate Chem.* **1991**, *2*, 1–12.
[13] A. M. Brun, A. Harriman, *J. Am. Chem. Soc.* **1994**, *116*, 10383–10393.
[14] S. Takenaka, K. Yamashita, M, Takagi, T. Hatta, A. Tanaka, O. Tsuge, *Chem. Lett.* **1999**, 319–320.
[15] A. Slama-Schwok, K. -P. Tealade-Fichou, J. -P. Vigneron, E. Taillandier, J. -M. Lehn, *J. Am. Chem. Soc.* **1995**, *117*, 6822–6830.
[16] B. Armitage, *Chem. Rev.* **1998**, *98*, 1171–1200, and references therein.
[17] K. Ito, S. Inoue, K. Yamamoto, S. Kawanishi, *J. Biol. Chem.* **1993**, *268*, 13221–13227.
[18] P. M. Cullis, M. E. Malone, L. A. Merson-Davies, *J. Am. Chem. Soc.* **1996**, *118*, 2775–2781.
[19] H. Sugiyama, I. Saito, *J. Am. Chem. Soc.* **1996**, *118*, 7063–7068.
[20] D. A. Dunn, V. H. Lin, I. E. Kochevar, *Biochemistry* **1992**, *31*, 11620–11625.
[21] S. J. Atherton, P. C. Beaumont, *J. Phys. Chem.* **1987**, *91*, 3993–3997.
[22] P. Fromherz, B. Rieger, *J. Am. Chem. Soc.* **1986**, *108*, 5361–5362.
[23] J. E. Rogers, S. J. Weiss, L. A. Kelly, *J. Am. Chem. Soc.* **2000**, *122*, 427–436.
[24] J. E. Rogers, T. P. Le, L. A. Kelly, *Photochem. Photobiol.* **2001**, *73–74*, 223–229.
[25] N. V. Eldho, J. Joseph, D. Ramaiah, *Chem. Lett.* **2001**, 438–439.
[26] J. Joseph, N. V. Eldho, D. Ramaiah, *J. Phys. Chem. B* **2003**, *107*, 4444–4450.
[27] D. Ramaiah, N. V. Eldho, J. Joseph, US Patent application no. US 2003045538A1 published on the web on 06/03/2003 at http://www.uspto.gov.
[28] L. S. Lerman, *J. Mol. Biol.* **1961**, *3*, 18–30.
[29] K. Tsukahara, N. Sawai, S. Hamada, K. Koji, Y. Onoue, T. Nakazawa, R. Nakagaki, K. Nozaki, T. Ohno, *J. Phys. Chem. B* **1999**, *103*, 2867.
[30] T. Wtanabe, K. Honda, *J. Phys. Chem.* **1982**, *86*, 2617.
[31] G. Scatchard, *Ann. N. Y. Acad. Sci.* **1949**, *51*, 660–672.
[32] J. D. McGhee, P. H. von Hippel, *J. Mol. Biol.* **1974**, *86*, 469–489.
[33] W. Adam, J. Cadet, F. Dall′Acqua, B. Epe, D. Ramaiah, C. R. Saha-Möller, *Angew. Chem.* **1995**, *107*, 91–94; *Angew. Chem. Int. Ed. Engl.* **1995**, *34*, 107–110.
[34] S. Boiteux, E. Gajewski, J. Laval, M. Dizdaroglu, *Biochemistry* **1992**, *31*, 106–110.
[35] B. Epe, M. Pflaum, M. Haring, J. Hegler, H. Rudiger, *Toxicol. Lett.* **1993**, *74*, 57–72.
[36] B. Epe, M. Haring, D. Ramaiah, H. Stopper, M. Abou-Elzahab, W. Adam, C. R. Saha-Moller, *Carcinogenesis* **1993**, *14*, 2271–2276.
[37] T. P. Le, J. E. Rogers, L. A. Kelly, *J. Phys. Chem. A* **2000**, *104*, 6778–6785.
[38] J. L. Sessler, B. Wang, A. Harriman, *J. Am. Chem. Soc.* **1995**, *117*, 704–714.
[39] J. W. Verhoeven, *Pure Appl. Chem.* **1990**, *62*, 1585–1596.
[40] M. R. Wasielewski, *Chem. Rev.* **1992**, *92*, 435–461.
[41] O. I. Aruoma, B. Halliwell, M. Dizdaroglu, *J. Biol. Chem.* **1989**, *264*, 13024–13028.
[42] E. Muller, S. Boieteux, R. P. Cunningham, B. Epe, *Nucleic Acids Res.* **1990**, *18*, 5969–5973.
[43] G. B. Schuster, *Acc. Chem. Res.* **2000**, *33*, 253–260.
[44] B. Giese, *Acc. Chem. Res.* **2000**, *33*, 631–636.
[45] M. C. Sajimon, D. Ramaiah, K. G. Thomas and M. V. George, *J. Org. Chem.* **2001**, *66*, 3182–3187.
[46] D. Ramaiah, M. Muneer, K. R. Gopidas, P. K. Das, N. P. Rath, M. V. George, *J. Org. Chem.* **1996**, *61*, 4240–4246.
[47] G. Weber, F. W. J. Teale, *Trans. Faraday Soc.* **1957**, *53*, 646–655.
[48] B. C. Baguley, E. -M. Falkenhang, *Nucleic Acids Res.* **1978**, *6*, 161–171.
[49] M. Saldit, S. N. Braunstein, R. D. Camerini-Otero, R. M. Franklin, *Virology* **1972**, *48*, 259–262.
[50] S. Boiteux, T. R. O′Conner, F. Lederer, A. Gouyette, J. Laval, *J. Biol. Chem.* **1990**, *265*, 3916–3922.
[51] H. Asahara, P. M. Wistort, J. F. Bank, R. H. Bakerian, R. P. Cunningham, *Biochemistry* **1989**, *28*, 4444–4449.
[52] S. Riazzudin in *Methods in Enzymology, Vol. 65* (Eds.: L. Grossman, K. Moldave), Academic Press, New York, **1980**, pp. 185–191.
[53] K. Akasaka, T. Suzuki, H. Ohuri, H. Meguro, Y. Shindo, H. Takahashi, *Anal. Lett.* **1987**, *20*, 1581–1594.
[54] N. V. Eldho, M. Saminathan, D. Ramaiah, *Synth. Commun.* **1999**, *29*, 4007–4014.
[55] N. Fisher, C. S. Franklin, E. N. Morgan, D. J. Tivey, *J. Chem. Soc.* **1958**, 1411.
[56] D. Rehm, A. Weller, *Ber. Bunsen-Ges.* **1969**, *73*, 834–836.
[57] A. Weller, *Phys. Chem.* **1982**, *133*, 93.
[58] Titan software version 1 from Wavefunction, Inc.; 18401, Von Karman, Suite 370, Irvine, CA 92612.
[59] A. Ledwith, *Acc. Chem. Res.* **1972**, *5*, 133.
[60] S. L. Murov, I. Carmichael, G. L. Hug, *Handbook of Photochemistry*, 2nd Ed., Marcel Dekker, New York, **1993**.

Received: March 11, 2003
Revised: August 20, 2003 [F4936]

